Proceedings of the XVIII ECSMGE 2024
GEOTECHNICAL ENGINEERING CHALLENGES
TO MEET CURRENT AND EMERGING NEEDS OF SOCIETY
© 2024 the Authors
ISBN 978-1-032-54816-6
DOI 10.1201/9781003431749-130
Open Access: www.taylorfrancis.com, CC BY-NC-ND 4.0 license

ECSMGE 24
XVIII EUROPEAN CONFERENCE ON SOIL MECHANICS AND GEOTECHNICAL ENGINEERING

Numerical modelling of unsaturated bentonite subjected to different hydro-mechanical stress paths

Modélisation numérique de bentonite insaturée soumise à différents chemins de contraintes hydromécaniques

C.E. Rodríguez*
UPC, Barcelona, Spain

A. Gens, R. Vasconcelos, J. Vaunat
UPC, CIMNE, Barcelona, Spain

**carlos.rodriguez.romero@upc.edu*

ABSTRACT: Bentonite-based materials such as MX-80 bentonite have been considered for their use as engineering barriers (EB) in deep radioactive waste geological repositories, mainly due to their low permeability, swelling pressure, and radionuclide retention properties. To ensure their integrity and to know their influence, different hydro-mechanical stress paths must be assessed. The European project BEACON (Bentonite Mechanical Evolution), addressed the behaviour of MX-80 bentonite subjected to different conditions including laboratory hydration tests carried out by EPFL (École Polytechnic Fédérale de Lausanne). For the fulfilment of the task, the constitutive response of the model is evaluated, decreasing the suction linearly to zero from its initial value simultaneously in the entire domain of analysis. A purely mechanical constitutive model calculation and no-flow conditions are enforced to probe the predictive power of the proposed numerical model. The paper presents a comparison between these numerical simulations and the laboratory test data showing satisfactory results.

RÉSUMÉ: Les matériaux à base de bentonite tels que la bentonite MX-80 ont été envisagés pour leur utilisation comme barrières techniques (EB) dans les dépôts géologiques profonds de déchets radioactifs, principalement en raison de leur faible perméabilité, de leur pression de gonflement et de leurs propriétés de rétention des radionucléides. Pour garantir leur intégrité et connaître leur influence, différents chemins de contraintes hydromécaniques doivent être évalués. Le projet européen BEACON (Bentonite Mechanical Evolution), a abordé le comportement de la bentonite MX-80 soumise à différentes conditions dont ces tests d'hydratation en laboratoire réalisés par l'EPFL (École Polytechnic Fédérale de Lausanne). Pour l'accomplissement de la tâche, la réponse constitutive du modèle est évaluée, en diminuant la succion linéairement jusqu'à zéro depuis sa valeur initiale simultanément dans tout le domaine d'analyse. Un calcul de modèle constitutif purement mécanique et des conditions d'absence de débit sont appliqués pour sonder le pouvoir prédictif du modèle numérique proposé. L'article présente une comparaison entre ces simulations numériques et les données d'essais en laboratoire montrant des résultats satisfaisants.

Keywords: MX-80 bentonite; hydro-mechanical; double porosity model; engineering barriers; stress path.

1 INTRODUCTION

The hydro-mechanical (HM) behaviour of bentonite-based materials has been extensively studied due to their potential use as sealing barriers in deep geological repositories for nuclear waste. These materials present appealing characteristics for their use, such as low hydraulic conductivity, swelling potential and sealing capacity. The bentonite is installed in an unsaturated state, but, due to environmental conditions, the barrier evolves to a saturated state. Because of its importance, it is necessary to verify their long-term behaviour to ensure their integrity under different hydro-mechanical stress paths. The Bentonite Mechanical Evolution project (BEACON), addressed the behaviour of samples of granular MX-80 bentonite subjected to different conditions such as those laboratory hydration tests carried out by EPFL (École Polytechnic Fédérale de Lausanne).

The occurrence of an active interaction between fabric and microfabric of active clays due to the physicochemical processes taking place at the particle level (Gens and Alonso, 1992) restricts the use of single-porosity formulations. In this respect, the development of mechanical constitutive models by Alonso et al., (1999) and Sánchez et al., (2005) considering the existence of two-pore structural levels

constituted a crucial enhancement of previous constitutive formulations for unsaturated clayey soils. In this work, the modelling is performed using this double-porosity model (DPM).

2 DESCRIPTION OF THE CONSTITUTIVE MODEL

The HM formulation requires a set of constitutive laws for dealing with the HM coupled processes that take place in geotechnical porous media.

An unsaturated soil is usually treated as a porous multi-phase medium composed of solid grains, water (as liquid water or vapour in the gas phase) and air (as dry air or dissolved in the liquid phase) (Olivella et al., 1996). Three-phase diagrams representing a soil element as a double porosity medium are shown in Figure 1. It can be easily noted that the volume of voids in the soil (V_p) is the sum of the volume occupied by macro-pores (V_{pM}) and micro-pores (V_{pm}). The volume of microstructure (V_m) includes the volume of the intra-aggregate pores (micro-pores) and the volume occupied by the solid phase (V_s).

Porosities (ϕ and ϕ_m) and void ratios (e and e_m) for the two porous media (the soil and the clay aggregate) are defined as:

$$\phi = \frac{V_p}{V} = \frac{V_{pm}}{V} + \frac{V_{pM}}{V} = \bar{\phi}_m + \bar{\phi}_M \tag{1}$$

$$\phi_m = \frac{V_{pm}}{V_m} \tag{2}$$

where $\bar{\phi}_m$ and $\bar{\phi}_M$ are the pore volume fractions associated with microstructure and macrostructure, respectively (Ruiz, 2020).

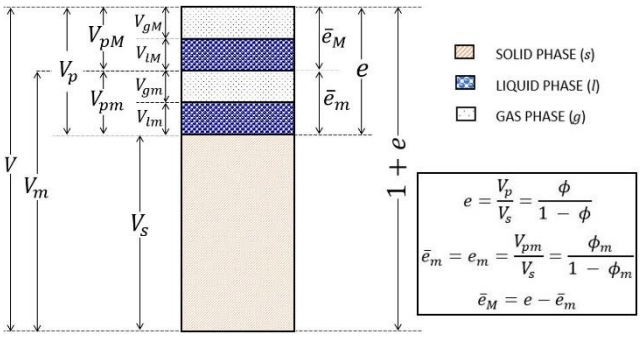

Figure 1. Phase diagram of a double structure unsaturated medium.

2.1 Mechanical model

In the current double porosity approach, the well-known BBM model (Alonso et al., 1990) is used for the macrostructural constitutive equation; the evolution of the yield surface in the stress space is dependent on the stress state, history variables and macro suction. The yield function for a general state, F_{LC}, in terms of the stress invariants (p, J, θ), is defined as:

$$F_{LC} = 3J^2 - M_F^2 \left(\frac{g_F(\theta)}{g_F\left(-\frac{\pi}{6}\right)} \right)^2 (p + p_s)(p_0 - p) = 0 \tag{3}$$

where M_F is the slope of the critical state line; g_F is a function of Lode's angle (θ); p_s expresses the dependence of the shear strength on macro suction and temperature; and p_0 is the apparent non-saturated pre-consolidation pressure that defines the Loading-Collapse (LC) locus in the $p: s_M$ plane according to

$$p_0 = p_c \left(\frac{p_0^*}{p_c} \right)^{\frac{\lambda(0) - \bar{\kappa}_M}{\lambda(s_M) - \bar{\kappa}_M}} \tag{4}$$

where p_0^* is the pre-consolidation pressure at saturation; p_c is a reference pressure; $\lambda(0)$, $\lambda(s_M)$ are the macro-structural compressibility at saturated and non-saturated conditions, respectively; and $\bar{\kappa}_M$ is the elastic stiffness parameter at macro for changes in the mean stress, p.

The microstructural mechanical behaviour is described by the following nonlinear elastic relationship:

$$K_m = \frac{1 + e_m}{\kappa_m} p_m \tag{5}$$

where K_m is the microstructural bulk modulus, p_m the effective mean stress acting on the microstructure and κ_m a model parameter.

It is assumed that microstructural volumetric deformation is fully reversible but can generate plastic deformation at macrostructural level ($\dot{\varepsilon}^p_{M,\beta}$) and is defined by:

$$\dot{\varepsilon}^p_{M,\beta} = f_\beta(\dot{\varepsilon}^e_m) \tag{6}$$

where f_β defines a pair of coupling functions dependent on the degree of compactness of macro-structure (μ_β) and on the sign of the mean effective stress increment at the micro-structural domain $(\dot{p}_m)$

$$f_\beta = \begin{cases} f_{MC}^{(1)} + \left(f_{MC}^{(0)} - f_{MC}^{(1)}\right)(1 - \mu_\beta)^{n_{MC}} if\ \dot{p}_m > 0 \\ f_{MS}^{(1)} + \left(f_{MS}^{(0)} - f_{MS}^{(1)}\right)(1 - \mu_\beta)^{n_{MS}} if\ \dot{p}_m < 0 \end{cases} \tag{7}$$

$f_{MC}^{(0)}$, $f_{MC}^{(1)}, n_{MC}$ and $f_{MS}^{(0)}$, $f_{MS}^{(1)}, n_{MS}$ are model parameters that define the coupling function in micro-structural contraction (*MC*) and micro-structural swelling (*MS*) paths, respectively.

2.2 Hydraulic model

Volumetric advective fluxes are formulated for the macro-structural domain, since the liquid and gas advective fluxes through micro-pores have been neglected. Therefore, the generalized Darcy's law ($\boldsymbol{q}_{\alpha M}$) for the α phase (liquid, l; gas, g) in expansive clays can be expressed as:

$$\boldsymbol{q}_{\alpha M} = -\boldsymbol{k}_M \frac{k_{r\alpha M}}{\mu_{\alpha M}} (\nabla P_{\alpha M} - \rho_{\alpha M} \boldsymbol{g}) \quad (8)$$

The intrinsic permeability tensor for the macrostructure, $\boldsymbol{k}_M$, is only dependent on its pore structure, according to the modified Kozeny-Carman equation:

$$\boldsymbol{k}_M = \boldsymbol{k}_{0,M} \frac{\bar{\phi}_M^3}{(1-\bar{\phi}_M)^2} \frac{(1-\bar{\phi}_0)^2}{\bar{\phi}_0^3} \quad (9)$$

$\bar{\phi}_0$ is the pore fraction for which the reference intrinsic permeability tensor $\boldsymbol{k}_{0,M}$ is estimated. The phase relative permeability, $k_{r_\alpha M}$, expresses the dependence of hydraulic permeability on the degree of saturation of the macrostructure. The decrease in liquid permeability with the reduction of the liquid saturation in macro-pores is defined through the following exponential function:

$$k_{r_l M} = A_{rl} \left(S_{el,M}\right)^{\lambda_r} \quad (10)$$

where the effective degree of saturation of macrostructure, $S_{el,M}$, is defined by:

$$S_{el,M} = \frac{S_{lM} - S_{lr,M}}{S_{ls,M} - S_{lr,M}} \quad (11)$$

in which S_{lM}, $S_{lr,M}$, $S_{ls,M}$ are the current, the residual and the maximum degree of saturation of the macrostructure, respectively; A_{rl}, λ_r are model parameters.

The water retention curve (WRC) of a porous medium relates its water content (or degree of saturation) to the pore-water potential (suction). Due to the assumption that micro-pores may be unsaturated, it is also necessary to define hydraulic constitutive laws for the microstructure by the definition of a WRC for this pore domain as well. In CODE_BRIGHT the water retention capacity of a porous medium is described by a modified van Genuchten law, as follows:

$$S_{el,\beta} = \left(1 + \left(\frac{s_\beta}{P}\right)^{\frac{1}{1-\lambda_{r\beta}}}\right)^{-\lambda_{r\beta}} \cdot \left(1 - \frac{s_\beta}{P_{d,\beta}}\right)^{\lambda_{d\beta}} \quad (12)$$

where s_β is the matric suction; $\lambda_{r\beta}$, $\lambda_{d\beta}$ are model parameters; P is a parameter related to the pore-air entry value dependent on temperature; and $P_{d,\beta}$ is the suction value at fully dry conditions.

Hydraulic equilibrium between the two structural levels is not assumed, which leads to a local exchange of mass of water and air between micro- and macro-pores. Sánchez, (2004) and Gens et al., (2011) proposed that the pore-water transferred between microstructure and macrostructure (Γ^w) is proportional to the difference in micro (s_m) and macro (s_M) suctions, that is,

$$\Gamma^w = \gamma^w (s_m - s_M) \quad (13)$$

The leakage parameter, γ^w, is related to the geometric characteristics of the porous media (Sánchez, 2004; Alonso and Navarro, 2005).

3 DESCRIPTION OF THE TEST

Tests were performed using a high-pressure oedometric cell that allows keeping the volume constant while measuring the axial load. Water is supplied from the bottom and top bases of the oedometric cell with a constant pressure of 20 kPa. The cell is made of stainless steel and holds an oedometric ring with height of 12.5 mm and diameter of 35.0 mm. The tested material is granular MX-80 bentonite with an initial void ratio in the range of 0.83-0.85 and a total suction is 110 MPa.

Path 1 (A-B-C-D) consisted on a hydration phase under constant vertical stress of 21 kPa. Path 2 (A-B'-D) also consisted of a hydration phase but at constant-volume conditions. Vertical stresses in both tests were increased in steps up to 20 MPa once full saturation was reached (Figure 2). Additional details of the test are provided in Ferrari et al., (2022).

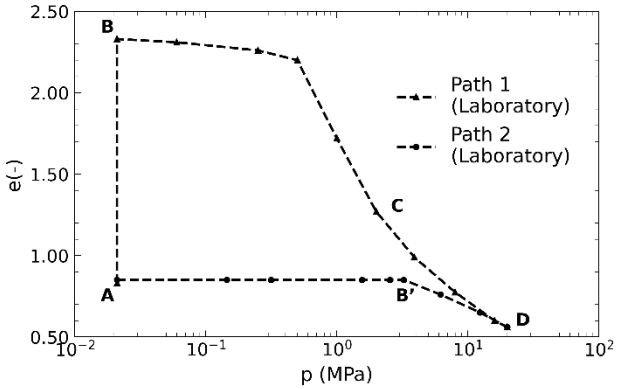

Figure 2. Hydro-mechanical stress paths under constant axial stress and constant volume conditions.

4 MODEL PARAMETERS

The HM parameters required in the numerical modelling were fitted using the experimental data in the literature (Seiphoori et al., 2014, 2015) and by back-calculating the results of the tests.

However, some other model parameters had to be calibrated during the modelling of this modelling task to fit the model predictions to the data from the laboratory tests. The main input parameters used to simulate the hydration tests are listed in Table 1.

Table 1. Main HM parameters for MX-80 bentonite.

Water Permeability Macro			
$k_{M,0}$	$[m^2]$	4e-21	Eq. (9)
$\bar{\phi}_{M,0}$	$[-]$	0.20	Eq. (9)
A_{rl}	$[-]$	1.0	Eq. (10)
λ_{rl}	$[-]$	6.0	Eq. (10)
Local Water Transfer			
γ^w	$\frac{kgs^{-1}m^{-3}}{MPa}$	5e-03	Eq. (13)
WRC (Macro)			
P_0	$[MPa]$	12.0	Eq. (12)
λ_{rM}	$[-]$	0.55	Eq. (12)
P_{dM}	$[-]$	1e27	Eq. (12)
λ_{dM}	$[-]$	3.90	Eq. (12)
WRC (micro)			
P_0	$[MPa]$	90.0	Eq. (12)
λ_{rm}	$[-]$	0.65	Eq. (12)
P_{dm}	$[-]$	1e27	Eq. (12)
λ_{dm}	$[-]$	0.8	Eq. (12)
Expansive Behaviour			
$\bar{\kappa}_M$	$[-]$	0.19e-4	Eq. (4)
$\bar{\kappa}_s$	$[-]$	0.28e-2	Eq. (4)
p_0^*	$[MPa]$	2.5	Eq. (4)
$\lambda(0)$	$[-]$	0.3	Eq. (4)
$f_{MS}^{(0)}$	$[-]$	4.0	Eq. (9)
$f_{MS}^{(1)}$	$[-]$	0.0	Eq. (9)
n_{MS}	$[-]$	2.0	Eq. (9)

5 NUMERICAL RESULTS AND DISCUSSION

A cubic sample of expansive soil, with a volume of 1.0 cm^3, was selected to represent the geometry. The tests were modelled by means of the finite element code CODE_BRIGHT. The generated mesh is composed of 125 identical hexahedral elements. The suction is decreased linearly to zero from its initial value simultaneously in the entire domain of analysis. It is a purely mechanical constitutive model calculation and no flow conditions are enforced.

In the wetting path at constant load conditions ("free swelling"), the confining pressure is applied on the upper surface and the four lateral surfaces. Under such conditions, vertical displacements (in the z-axis direction) are not allowed at the lower surface.

In contrast, in the isochoric condition path, the vertical displacements are restricted in all surfaces of the volume until the suction is reduced to a value of 0.

The FE mesh and three orthogonal views with the applied mechanical boundary conditions for the wetting path under unconfined (free swelling) and confined (isochoric) conditions are displayed in Figure 3.

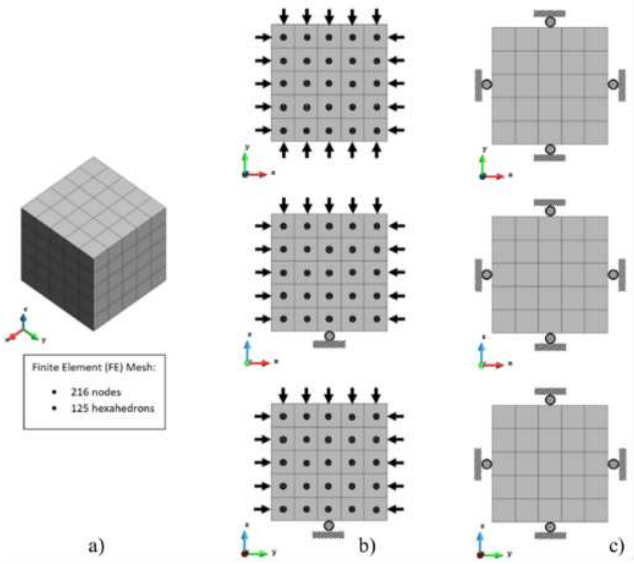

Figure 3. Schematic representation of the modelled geometry (FE mesh) of a cubic element of expansive soil together with the mechanical boundary conditions under (b) unconfined and (c) confined swelling/shrinkage evolution.

5.1 Analysis of stress path 1

In path 1 the swelling of the clay aggregates leads to an increase in macro-porosity, which produces a global expansion of the soil element (increase in total porosity). It can be seen that during the swelling stage (A-B) the LC curve moves to the left (Figure 4) in response to the plastic swelling strains taking place in

the macrostructure. This is due to the low isotropic stress ratio p/p_0. When this ratio is low, it implies a dense packing of the clay aggregates and, under this condition, the micro-structural swelling (MS path) affects strongly the global arrangements of clay aggregates, inducing large macro-structural plastic strains and a macro-structural softening.

After saturation, subsequent loading (B-D) takes the LC again to the right to the final load value of approximately 8.0 Mpa (Figure 5). During the subsequent loading (B-D), under saturated conditions, the deformation of the macrostructure is significant but it is not due to micro-structural strains that are now quite small.

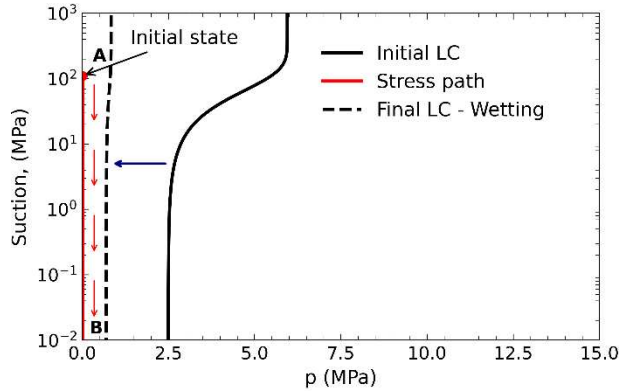

Figure 4. Schematic representation of Path 1. Wetting at constant confining pressure (in the p:s_M plane).

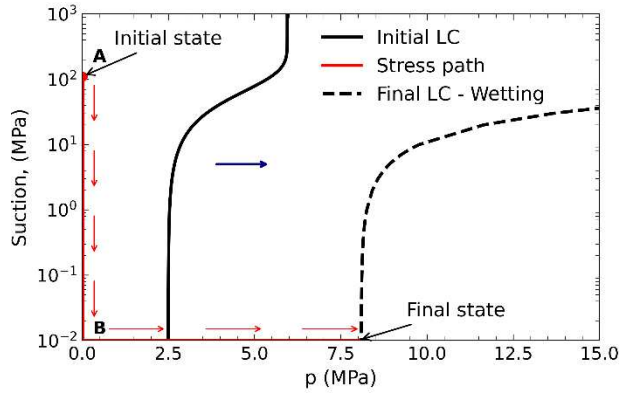

Figure 5. Schematic representation of Path 1. Subsequent load after wetting (in the p:s_M plane).

5.2 Analysis of stress path 2

For the isochoric test, since the modelling of these stress paths is merely constitutive, the value of the macro-structural liquid pressure is prescribed at all nodes of the FE mesh. Null displacements were prescribed at all nodes of the mesh to reproduce the test under costant volume conditions. The initial location of the LC curve is presented along with the different positions of the LC yield curve during the performance of the test (Figure 6). Initially, the stress increases due to the development of swelling pressure. Once the LC yield surface is reached, the vertical stress drops to compensate for the tendency of the macrostructure to collapse so that the sample length is maintained constant. It can be seen that during the wetting stage (A-B') the LC curve moves slightly to the right in response to macro-structural hardening. In the final stage (B'-D), the reduction of pores can be observed; it is related to the progressive increase of vertical stress (Figure 7). Comparing the numerical predictions with the experimental results in path 2, a good agreement is obtained.

Figure 8 shows the comparison between model and experimental results for paths 1 and 2. As can be seen, the agreement with experimental data is reasonably satisfactory although some departures from observations can be noted. Specifically, the following features have been correctly reproduced: large swelling strains upon wetting under low applied stresses, a clearly defined yield point when loading after wetting, stress path dependency comparing the swelling pressure test and the swell-load test (although the void ratio difference is overestimated by the model) and a realistic value of swelling pressure. In contrast, the convergence of the loading compression lines is not captured by the model.

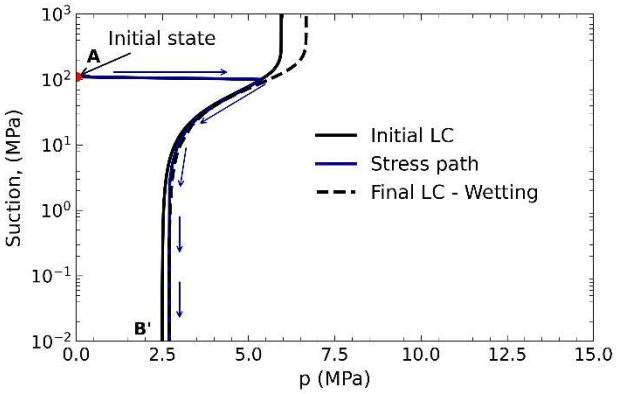

Figure 6. Schematic representation of Path 2. Wetting at constant volume conditions (in the p:s_M plane).

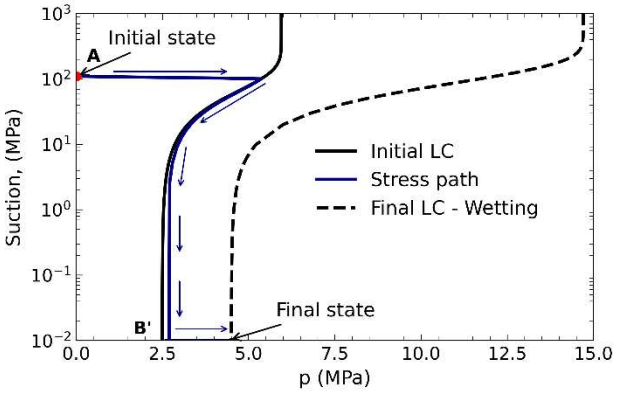

Figure 7. Schematic representation of Path 2. Subsequent load after wetting (in the p:s_M plane).

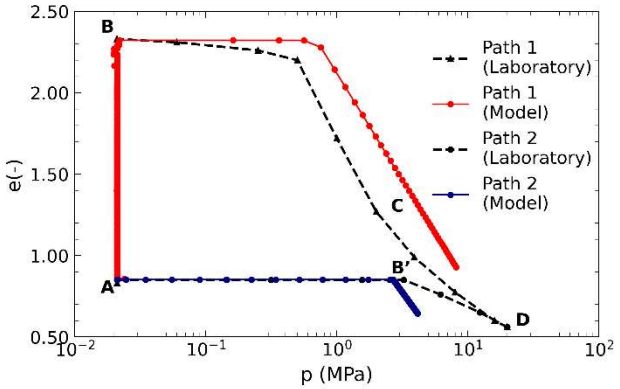

Figure 8. Laboratory and modelling path results.

6 CONCLUSIONS

The capabilities of the double-porosity model to reproduce the swelling response of expansive materials under hydration conditions have been evaluated through the performance of constitutive problem analyses. The overall variation of the void ratio along the two stress paths has been satisfactorily reproduced by the constitutive model, however, the convergence of the compression lines is not captured.

ACKNOWLEDGEMENTS

The work presented has been developed in the frame-work of the Bentonite Mechanical Evolution Project (BEACON). The project receives funding from the Euratom research and training programme 2014-2018 under grant agreement No 745942. The support of Conacyt (Id. no. 710153) to the first author is also gratefully acknowledged.

REFERENCES

Alonso, E.E., Gens, A., Josa, A., (1990). A constitutive model for partially saturated soils. *Géotechnique*, 40, pp. 405–430. https://doi.org/10.1680/geot.1990.40.3.405.

Alonso, E.E., Vaunat, J., Gens, A., (1999). Modelling the mechanical behaviour of expansive clays. *Engineering Geology,* 54, pp. 173-183. https://doi.org/10.1016/S0013-7952(99)00079-4.

Alonso, E.E. and Navarro, V., (2005). Microstructural model for delayed deformation of clay: loading history effects, *Canadian Geotechnical Journal*, 42, pp. 381-392. https://doi.org/10.1139/t04-097.

Ferrari, A., Bosch, J.A., Baryla, P., Rosone, M., (2022). Volume change response and fabric evolution of granular MX80 bentonite along different hydro-mechanical stress paths, *Acta Geotechnica*, 17, pp. 3719-3730. https://doi.org/10.1007/s11440-022-01481-0.

Gens, A., Alonso, E.E., (1992). A framework for the behaviour of unsaturated expansive clays. *Canadian Geotechnical Journal,* 29, pp. 1013-1032. https://doi.org/10.1139/t92-120.

Gens, A., Valleján, B., Sánchez, M., Imbert, C., Villar, M.V. and Van Geet, M., (2011). Hydromechanical behaviour of a heterogeneous compacted soil : experimental observations and modelling, *Géotechnique*, (5), pp. 367–386. https://doi.org/10.1680/geot.SIP11.P.015.

Olivella, S., Gens, A., Carrera, J. & Alonso, E.E., (1996). Numerical formulation for a simulator (CODE_BRIGHT) for the coupled analysis of saline media, *Engineering Computations*, 13 (7), pp. 87-112. https://doi.org/10.1108/02644409610151575.

Ruiz, D., (2020). *Hydro-mechanical analysis of expansive clays constitutive and numerical modelling*. PhD Thesis, Technical University of Catalonia (UPC). Available at: https://upcommons.upc.edu/handle/2117/192447.

Sánchez, M., (2004). *Thermo-hydro-mechanical coupled analysis in low permeability media*. PhD Thesis, Technical University of Catalonia (UPC). Available at: https://upcommons.upc.edu/handle/2117/107703.

Sánchez, M., Gens, A., Guimarães , L. do N., Olivella, S., (2005). A double structure generalized plasticity model for expansive materials. *International Journal for Numerical and Analytical Methods in Geomechanics*. 29, 751-787. https://doi.org/10.1002/nag.434.

Seiphoori, A., Ferrari, A. and Laloui, L., (2014). Water retention behaviour and microstructural evolution of MX-80 bentonite during wetting and drying cycles. *Géotechnique*, 64(9), pp.721-734. http://dx.doi.org/10.1680/geot.14.P.017.

Seiphoori, A., (2015). Thermo-hydro-mechanical characterisation and modelling of Wyoming granular bentonite. NAGRA, Switzerland, Technical Report 15-05.

Vasconcelos, R., (2021). *A double-porosity formulation for the THM behaviour of bentonite-based materials*, PhD Thesis, Technical University of Catalonia (UPC). Available at: https://upcommons.upc.edu/handle/2117/349570.

INTERNATIONAL SOCIETY FOR SOIL MECHANICS AND GEOTECHNICAL ENGINEERING

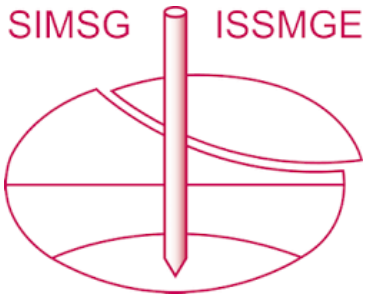

This paper was downloaded from the Online Library of the International Society for Soil Mechanics and Geotechnical Engineering (ISSMGE). The library is available here:

https://www.issmge.org/publications/online-library

This is an open-access database that archives thousands of papers published under the Auspices of the ISSMGE and maintained by the Innovation and Development Committee of ISSMGE.

The paper was published in the proceedings of the 18th European Conference on Soil Mechanics and Geotechnical Engineering and was edited by Nuno Guerra. The conference was held from August 26th to August 30th 2024 in Lisbon, Portugal.